Journal of Photochemistry and Photobiology A: Chemistry 219 (2011) 180–187

Contents lists available at ScienceDirect

Journal of Photochemistry and Photobiology A: Chemistry

journal homepage: www.elsevier.com/locate/jphotochem

Highly efficient dye-sensitized solar cells based on nitrogen-doped titania with excellent stability

Wei Guo [a], Liqiong Wu [a], Zhuo Chen [a], Gerrit Boschloo [b], Anders Hagfeldt [b], Tingli Ma [a,*]

[a] State Key Laboratory of Fine Chemicals, Dalian University of Technology, School of Chemical Engineering 158 Zhongshan Rd. Box 40, Dalian 116012, PR China
[b] Department of Physical and Analytical Chemistry, Uppsala University, Box 259, 751 05 Uppsala, Sweden

ARTICLE INFO

Article history:
Received 26 July 2010
Received in revised form
20 December 2010
Accepted 6 January 2011
Available online 13 January 2011

Keywords:
N-doped titania
Dye-sensitized solar cell
Electron transport
Photovoltaic performance

ABSTRACT

A series of nitrogen-doped and undoped TiO_2 nanocrystals was prepared by several simple methods. Needle-like N-doped TiO_2 nanocrystals and nanoparticles were obtained from commercial TiO_2 powders. Several dye-sensitized solar cells (DSCs) were fabricated based on N-doped and undoped TiO_2 electrodes. The N-doped DSCs achieved a high conversion efficiency of 10.1% and 4.8% using an organic electrolyte and an ionic liquid electrolyte, respectively. Systemic investigations were carried out on the properties of N-doped and undoped TiO_2 powders, films, and DSCs. The electron transport time and electron lifetime were investigated by intensity-modulated photocurrent and photovoltage spectroscopy (IMPS/IMVS). Moreover, the electron injection of N-doped DSCs was studied by surface photovoltage spectroscopy (SPS). The synergetic effect of higher dye uptake, faster electron transport and higher photovoltage contributes to a higher conversion efficiency of N-doped DSCs. The stability test also demonstrated that the photodegradation of the DSCs was not accelerated and the DSC system was stabilized by the introduction of nitrogen into the TiO_2 photoelectrode. These results indicate that the N-doped TiO_2 nanocrystals prepared by our approach from commercial TiO_2 are ideal semiconductor materials for DSCs.

1. Introduction

Since Grätzel et al. developed a new type of solar cell based on nanocrystalline porous titania electrode, dye-sensitized solar cells (DSCs) have attracted considerable interest as a low-cost alternative to conventional silicon solar cells [1–3]. However, further improving the energy conversion efficiency of DSCs is important for successful commercialization. The semiconductor oxide photoelectrode is known to be one of the key components that affects the energy conversion efficiency of DSCs. TiO_2 is a typical semiconductor oxide material for photoelectrodes. Several semiconductor oxide materials, such as Nb_2O_5 [3,4], ZnO [5], SnO_2 [6], WO_3 [7], $SrTiO_3$ [8], CeO_2 [9], Zn_2SnO_4 [10,11], FeS [12], and NiO [13,14], have also been applied in developing DSCs. However, the conversion efficiencies of these DSCs did not prove to be high enough. Recently, studies on modifying pure TiO_2 with metal doping, i.e., using Cr and Nb, have been conducted. Han et al. [15] reported a Cr-doped TiO_2 film that was used as a blocking layer in DSCs to repress electron recombination, thereby enhancing the efficiency of the DSC by 18.3%. Kim et al. [16] reported that Nb-doped TiO_2 thin film deposited on fluorine-doped tin oxide conducting glass (FTO glass) functions both as a blocking layer and an ancillary transparent conducting oxide layer in DSCs. The efficiency of the DSC incorporated with Nb-doped TiO_2 layer was enhanced by 4.1% as compared to that incorporated with undoped TiO_2 layer. However, the photovoltaic performance of the DSCs based on these semiconductor materials remains low. Moreover, oxygen deficiencies exist in the pure TiO_2 crystal structure [17–19]. It is well known that oxygen deficiency can induce visible light absorption leading to the oxidation of iodide or dye by photogenerated holes [20]. Such deficiencies are possible causes of the shortened lifetime of DSCs. In order to solve the problems mentioned above, we have developed a DSC system based on N-doped TiO_2, which successfully achieved high energy conversion efficiency [21–23]. However, in this previous work, we only compared three DSCs based on N-doped TiO_2, pure P25, and Ti-Nanoxide D (Solaronix Co., Ltd.) electrodes. In order to understand the effect of N-doped TiO_2 on the DSCs system and clarify the mechanism of obtaining high energy conversion efficiency, we perform further investigations of N-doped and undoped TiO_2.

In this paper, a simple method was used to prepare the needle-like N-doped TiO_2 nanocrystals from commercial TiO_2 powders. We carried out investigations of the properties of the N-doped and undoped TiO_2 powders, films, and solar cells. Furthermore, the electron injection of N-doped DSCs was studied by surface photovoltage spectroscopy (SPS). Electron transport time and electron lifetime in the N-doped and undoped DSCs were analyzed by intensity-modulated photocurrent and photovoltage spectroscopy

* Corresponding author. Tel.: +86 411 39893820; fax: +86 411 39893820.
E-mail address: tinglima@dlut.edu.cn (T. Ma).

1010-6030/$ – see front matter © 2011 Elsevier B.V. All rights reserved.
doi:10.1016/j.jphotochem.2011.01.004

(IMPS and IMVS). The stability tests of the N-doped films and the DSCs were performed at ambient temperature with changing seasons.

2. Experimental

2.1. Preparation of nanocrystalline TiO_2 powders

Commercially available ST-01 (Ishihara Sangyo Kaisha, Ltd.) and P25 (Degussa) TiO_2 powders were used to prepare N-doped TiO_2 through a simple dry method. In brief, nanocrystalline N-doped ST-01 and N-doped P25 powders were prepared by sintering pure TiO_2 powders at 500 °C for 3 h under dry N_2 and NH_3 gas flow. For comparison, pure ST-01 was also treated under the same conditions without nitrogen source and the obtained sample was denoted as undoped ST-01. Pure ST-01 powder was sintered at 450 °C for 30 min in atmospheric air, denoted as S-ST-01. A series of N-doped ST-01 with different N amounts was prepared by controlling the ratio of N_2/NH_3 in the gas flow, which were designated as NT-1, NT-2, NT-3, and NT-4. Among them, the DSCs based on NT-3 electrodes offered the highest energy conversion efficiency. Therefore, NT-3 was used in the following discussions and denoted as the N-doped ST-01.

The N-doped TiO_2 powders were prepared by a modified wet method as follows: the hydrolysis of titanium tetraisopropoxide (Wako 97%) was carried out in aqueous ammonia (Wako 28%). A 25 ml aliquot of titanium tetraisopropoxide was added dropwise to 100 ml aqueous ammonia under vigorous stirring in an ice bath. The white precipitate was formed and filtered in a funnel and washed by water. After drying at 80 °C for 1 h, the powder was sintered at 450 °C for 4 h (1 °C/min). The yellow powder obtained was denoted as N-doped A. Undoped TiO_2 was prepared by the same process, except the hydrolysis of titanium tetraisopropoxide was carried out in deionized water, the obtained white powder was denoted as undoped A.

2.2. Preparation of N-doped and undoped TiO_2 photoelectrodes

The screen-printable N-doped and undoped TiO_2 colloidal pastes were prepared according to the procedure developed by our group [24]. Briefly, polyethylene glycol (PEG 600) was used as the dispersion medium for the paste without any other binder. A screen-printing technique was used to fabricate the films. Firstly, the N-doped or undoped TiO_2 paste was printed on the FTO conducting glass (Asahi Glass Co., Ltd.; sheet resistance: 10 ohm/square). Secondly, the obtained film was dried at 200 °C for 10 min in atmospheric air. Afterwards, a scattering layer was coated on top of the films using a paste that was a mixture of the N-doped (or undoped) powders and the large particle (ST-41, 200 nm, Ishihara Sangyo Kaisha, Ltd.) TiO_2 powders in a 7:3 weight ratio. Then, the film was sintered at 500 °C for 30 min in atmospheric air. The film was immersed in 40 mM $TiCl_4$ solution for 30 min at 70 °C and then sintered at 500 °C for 30 min. After cooling down to 80 °C, the film was dipped into a dye solution of 5×10^{-4} M cis–bis(isothiocyanato)bis(2,2′-bipyridyl-4,4′-dicarboxylato)-ruthenium(II)-bis-tetrabutyl-ammonium (N719) dissolved in acetonitrile and 4-*tert*-butyl alcohol (volume ratio = 1:1) and kept at room temperature for 12 h. Finally, dye-sensitized N-doped and undoped TiO_2 photoelectrodes were prepared.

2.3. Fabrication of DSCs

The dye-sensitized TiO_2 electrode (thickness: 15 μm, area: 0.16 cm^2) and a platinized counter electrode were assembled to form a solar cell by sandwiching a redox (I^-/I_3^-) electrolyte solution. In this work, the organic electrolyte was composed of 0.03 M I_2, 0.06 M LiI, 0.6 M 1-butyl-3-methylimidazolium iodide (BMII), 0.1 M guanidinium thiocyanate, and 0.5 M 4-*tert*-butylpyridine (4TBP) in acetonitrile. In addition, the ionic liquid electrolyte consisted of 0.1 M LiI, 0.1 M I_2, 0.9 M BMII, and 0.5 M 4TBP dissolved in 1-ethyl-3-methylimidazolium tetrafluoroborate ($EMImBF_4$). In order to carefully compare the conversion efficiency and open-circuit voltage (V_{oc}) of the N-doped DSCs, we fabricated 36 pair cells of N-doped and undoped DSCs under the same conditions.

2.4. Photovoltaic measurement of DSCs

The current–voltage curves of the DSCs were obtained by applying an external bias to the cell and measuring the generated photocurrent under white light irradiation with a Keithley digital source meter (Keithley 2601, USA). The intensity of the incident light was 100 mW/cm^2, and the instrument was equipped with a 300 W solar simulator (Solar Light Co., Inc., USA) that served as the light source. The photon flux was determined by a power meter (Nova, Ophir Optronics Ltd.) and a calibration cell (BS-520, s/n 019, Bunkoh-Keiki Co., Ltd.). The photoelectrochemical current–voltage measurement of the N-doped and undoped ST-01 electrodes was performed using a BAS100B electrochemical analyzer in a single-compartment cell with quartz windows. A platinum wire and Ag/AgCl electrode in saturated KCl were used as the counter electrode and reference electrode, respectively. The working electrodes of N-doped ST-01 and undoped ST-01 electrodes were illuminated with a 300 W solar simulator (Solar Light Co., Inc., USA). The beam passed through a 420 nm filter to cut off wavelengths below 420 nm. The electrolyte selected in the present work was 0.1 M KI and 0.01 M K_2HPO_4/KH_2PO_4 buffers (pH 6.8) [25].

The SPS was measured using the surface photovoltage instrument (SKP5050, KP technology Ltd., UK). A monochromatic light was obtained by passing light from a 250 W halogen tungsten lamp through a double-prism monochromator. The SPS was obtained using the Kelvin probe method, wherein a vibrating Au reference electrode served as the second electrode situated above the photoelectrodes [26].The changes in contact potential difference (ΔCPD = surface photovoltage) were measured. This will reflect differences in the work function between the Au electrode and the photoelectrodes.

For measuring the IMPS and IMVS, a white light-emitting diode (Lumiled Luxeon Star 1W) was used as a light source at room temperature. The details were described elsewhere [27].

2.5. Stability test of the dye and the N-doped DSCs

Stability tests were performed on the dye adsorbed on the N-doped TiO_2 films and photoelectrodes of complete solar cells. The N719 dye-sensitized TiO_2 films were stored at ambient temperature for four years in Japan and China. The complete DSCs were assembled by sandwiching a 50 μm thick Surlyn film (spacer) between the N-doped or undoped ST-01 photoelectrodes (1×1 cm^2) and a platinized counter electrode. The electrolyte was introduced to the cell through a small hole drilled in the counter electrode by vacuum infusion. The DSCs were illuminated under sunlight for 109 days in Dalian, China from November 2008 to March 2009 at ambient temperature as the seasons changed. Afterwards, the sealed cells were disconnected. The dye adsorbed on the TiO_2 photoelectrodes mentioned above was desorbed in a mixed solution of water and ethanol (volume ratio = 1:1) containing 0.1 M NaOH. After that, the extracted dye solution was treated with 22.5 μl formic acid and then analyzed by UV–vis spectroscopy.

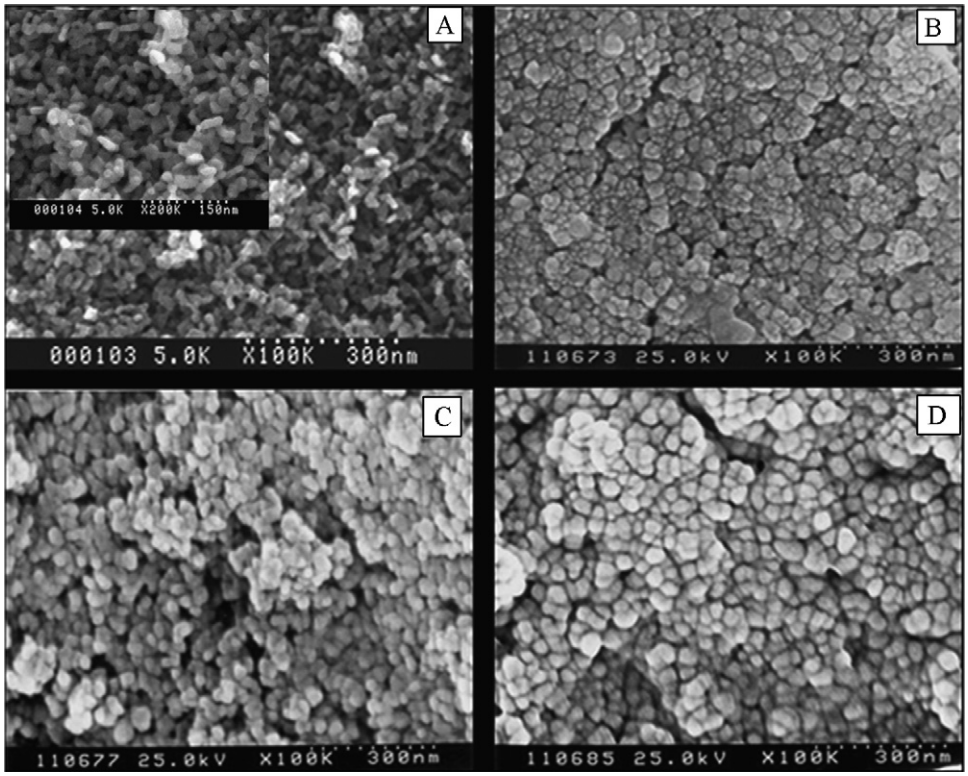

Fig. 1. Scanning electron micrographs of (A) N-doped ST-01 powders prepared by the dry method; (B) N-doped A film; (C) N-doped ST-01 film, and (D) undoped ST-01 film.

3. Results and discussion

3.1. Physical properties of N-doped and undoped TiO_2

The surface morphologies of the N-doped and undoped TiO_2 powders and films were characterized by scanning electron microscopy (SEM). As shown in Fig. 1a, the nanocrystal N-doped ST-01 powders exhibit a needle-like appearance with a particle size of $15 \times 30\,nm^2$. We can clearly observe this needle-like nanostructure from SEM image with high resolution (the inset of Fig. 1a). In contrast, the pure ST-01 powders as the starting material display a spherical morphology with a particle size of 10 nm. This result implies that the nanoparticle size and morphology can be effectively controlled by our doping approach. The BET (Brunauer-Emmett-Teller) analysis showed that the surface area of the N-doped ST-01 powders is $67\,m^2/g$. For the N-doped A prepared by the wet method, the particles also exhibit a spherical morphology with a particle size of 25 nm and a surface area of $60\,m^2/g$. Furthermore, both N-doped ST-01 and undoped ST-01 films show porous network surface structures in Fig. 1, whereas larger particle aggregates appear in the undoped ST-01 film.

Structural characterization of the N-doped A powders was performed by X-ray diffraction (XRD). The crystal phase of N-doped A powders is anatase (ESI† Fig. S1). Commercial ST-01 is also 100% anatase phase, and no rutile phase is observed after treatment with a dry method [21].

3.2. Optical properties of N-doped and undoped TiO_2

We used an integrating sphere setup to measure the UV–vis absorption spectra of the N-doped ST-01, N-doped P25, N-doped A, and undoped ST-01 powders. The results are shown in Fig. 2. No absorption peak for the undoped ST-01 is observable above 400 nm, whereas the N-doped ST-01, N-doped A, and N-doped P25 powders display a new absorption peak in the visible region from 400 to 500 nm. Furthermore, the absorption intensity of the N-doped ST-01 is higher than that of N-doped P25. Elemental analysis shows that the N dopant amounts of the N-doped ST-01 and P25 are *ca.* 2.49 at.% and *ca.* 0.98 at.%, respectively. This indicates that the N dopant amount of the N-doped ST-01 is higher than that of the N-doped P25. Fang et al. [28] reported that the N-doped TiO_2 powders obtained from TiO_2 xerogel powders, which were prepared by peptizing $Ti(OH)_4$, exhibit more obvious absorption in the visible-light region and possess a higher concentration of the substitutional nitrogen compared with the N-doped TiO_2 prepared from P25. These results imply that the starting materials directly affect the N doping amount of TiO_2 powders.

In addition, we investigated the absorption spectra of the N-doped ST-01 powders sintered in various gas atmospheres and at

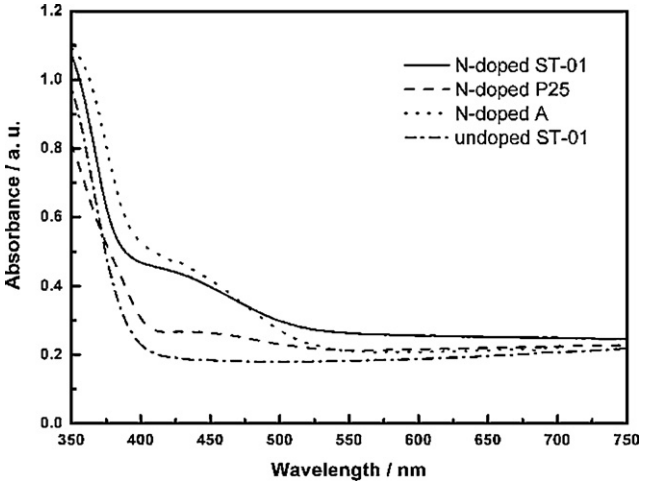

Fig. 2. UV–vis spectra of N-doped ST-01, N-doped P25, N-doped A, and undoped ST-01 powders.

different temperatures (ESI† Fig. S2). The results show that the absorption intensities of the N-doped ST-01 powders sintered in air, Ar, and N_2 atmospheres are almost identical. Furthermore, the absorption intensity is weakened as the sintering temperature increases. However, the peak notably still exists after sintering at 600 °C for 30 min. These results indicate that N-doped ST-01 has excellent thermostability, owing to a chemically bound N^- species within the crystalline TiO_2 lattice [21]. Burda et al. [29] reported that the nitrogen concentration of the N-doped TiO_2 decreases as the sintering temperature increases because the oxygen in air can substitute the doped nitrogen much faster above 400 °C.

3.3. Photoelectrochemical performance of DSCs

Fig. S3 (see ESI†) shows the photoelectrochemical performance of the DSCs fabricated using the NT-1, NT-2, NT-3, and NT-4 electrodes. The energy conversion efficiency of the NT-3 DSC is the highest among the four samples. We suggest that the nitrogen doping amount affects the photoelectrochemical property of solar cells, which is consistent with the results reported by Yang et al. [30]. A detailed effect of the nitrogen doping amount on the performance of DSCs will be discussed in another paper. In order to further improve the efficiency of the NT-3 DSC, optimization was performed with a coating of light-scattering TiO_2 layer on the NT-3 film, which is denoted as N-doped ST-01 in the following discussion. Fig. 3 and Table 1 shows the performance of DSCs based on N-doped and undoped TiO_2 electrodes using an organic electrolyte.

Interestingly, the commercial ST-01 film appears fully cracked, lowering the energy conversion efficiency of DSC to 2.7%. However, the crystallinity of the sintered ST-01 powders (S-ST-01 powders) at 450 °C has been improved, leading to the enhancement of the energy conversion efficiency of 5.6%. The undoped ST-01 film appears to be in good state. Hence, the energy conversion efficiency of the undoped ST-01 DSC significantly increases to 8.9%. When nitrogen was doped to the pure ST-01 powders, the N-doped ST-01 DSC achieves an efficiency of 10.1%. On the other hand, a good energy conversion efficiency of 8.6% was also attained by the DSCs based on the N-doped A electrode prepared by the wet method, with a higher photocurrent than that of undoped A. An efficiency enhancement of *ca.* 10% is clearly obtained after modification by N-doping in all three cases (Table 1).

Upon comparing 36 pairs of the N-doped and undoped ST-01 DSCs, 25 N-doped ST-01 DSCs show higher conversion efficiency, while 23 N-doped ST-01 DSCs show higher V_{oc}. With regard to the obtained higher V_{oc} for the N-doped DSCs, the surface photovoltage spectra was investigated and discussed in the following section. Moreover, the energy conversion efficiency of the DSCs based on an N-doped ST-01 electrode is higher than that of the DSCs based on an N-doped P25 electrode. This result is caused by the difference in the crystalline phase of the starting TiO_2 materials and the different nitrogen doping amounts. Therefore, the starting TiO_2 materials for nitrogen doping and the N dopant amount of N-doped TiO_2 are crucial for the energy conversion efficiency of DSCs based on N-doped TiO_2 electrodes.

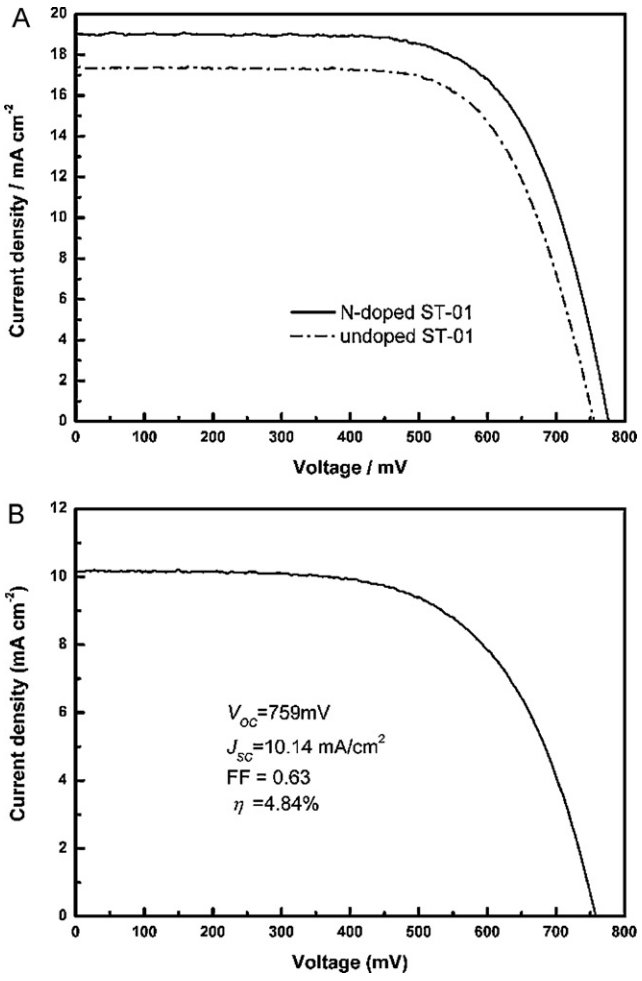

Fig. 3. Photocurrent–voltage curves of DSCs. (A) DSCs based on the N-doped and undoped ST-01 electrodes using an organic electrolyte. (B) DSCs based on the N-doped ST-01 electrode using an ionic liquid electrolyte.

In general, a volatile organic solvent in DSCs causes leakage of the electrolyte after prolonged use. Ionic liquids with non-volatility, non-flammability, and high ionic conductivity properties seem to be the most appropriate solvents used to solve such a problem. Therefore, the photovoltaic performance of DSCs based on N-doped TiO_2 electrode was studied using an ionic liquid electrolyte. Fig. 3(B) shows that the energy conversion efficiency of DSCs based on an N-doped ST-01 electrode can reach 4.8%.

In order to further identify the factors that led to a higher photocurrent of N-doped DSCs, the electrochemical properties of TiO_2 electrodes were studied without dye under visible light illumination. Representative voltammograms are shown in Fig. 4. The photocurrent is significantly enhanced for the N-doped ST-01 electrode compared to that of the undoped ST-01 electrode. The result is consistent with the electrochemical property of the N-doped TiO_2

Table 1
Performance of the DSCs based on the N-doped and undoped TiO_2 electrodes using organic electrolyte solution.

Titania electrode	V_{OC} (mV)	J_{SC} (mA/cm^2)	FF (%)	η (%)
N-doped ST-01	778 ± 10	19.05 ± 0.07	0.68 ± 0.01	10.1 ± 0.2
Undoped ST-01	756 ± 13	17.40 ± 0.10	0.68 ± 0.01	8.9 ± 0.3
S-ST-01	700 ± 10	12.30 ± 0.10	0.65 ± 0.01	5.6 ± 0.2
Commercial ST-01	741 ± 15	6.66 ± 0.03	0.56 ± 0.01	2.7 ± 0.2
N-doped P25	789 ± 10	14.66 ± 0.13	0.69 ± 0.01	8.0 ± 0.2
Commercial P25	769 ± 15	13.58 ± 0.07	0.68 ± 0.01	7.1 ± 0.2
N-doped A	784 ± 8	15.58 ± 0.17	0.68 ± 0.01	8.3 ± 0.3
Undoped A	747 ± 7	14.80 ± 0.17	0.65 ± 0.01	7.2 ± 0.3

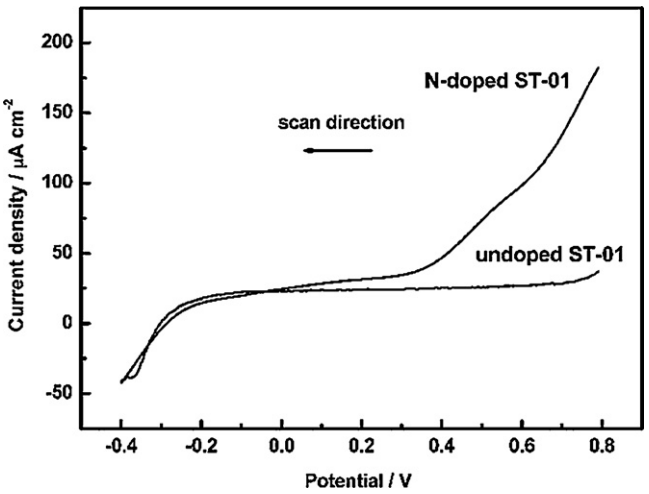

Fig. 4. *I–V* characteristics of the N-doped ST-01 and undoped ST-01 electrodes. The electrodes were mounted in a three-electrode setup and illuminated from the substrate/electrolyte interface in a 0.1 M aqueous electrolyte (pH = 6.8). The scan rate was 1 mV/s.

electrode reported by Lindquist et al. They demonstrated that the photocurrent can be increased by about 200 times for the best N-doped TiO_2 electrode compared to the behavior of undoped TiO_2 electrode [25]. However, the photocurrent generated by N-doped TiO_2 electrodes without dye only exceeded 100 μA/cm^2. This result cannot explain the difference in short-circuit current between the complete N-doped and undoped DSCs. The difference of photocurrent in the complete N-doped DSCs was larger than 1 mA/cm^2. It is well known that a larger surface area of the film can increase the amount of dye uptake and further lead to an increase in the energy conversion efficiency of DSCs. We further investigate the amount of dye absorbed on N-doped ST-01 and undoped ST-01 electrode. We observed a higher dye uptake on the N-doped ST-01 film (12.3×10^{-8} mol/cm^2), compared with that for undoped one (9.13×10^{-8} mol/cm^2). Our previous work also suggests that the enhanced light absorption of nitrogen-doping is an important factor in the good performance of solar cells [21].

3.4. Surface photovoltage of DSCs

The mechanism of higher open circuit voltage in the N-doped DSCs is an important part of understanding the basic process of electron injection. In any photovoltaic cell, the photovoltage is determined by the light-induced difference in Fermi levels (E_F). For DSCs, these Fermi levels can be identified with the redox potential of the I^-/I_3^- solution and the conduction band edge of the electron-conducting semiconductor [31]. Therefore, the photovoltage increases when the energy difference between the two levels increases. Since the redox couple I^-/I_3^- is fixed in the DSCs, different electron-conducting semiconductors cause a change in the open-circuit photovoltage. The SPS is a well-established and contactless method that can provide detailed and quantitative information on bulk properties (e.g., bandgap and type) and can be used for measuring energy levels [32].

Fig. 5A shows the SPS results of N-doped and undoped ST-01 film without dye, with the typical response band close to 350 nm originating from the band-band electron transition of TiO_2. In the visible light region at about 430 nm, an impurity level exists from where photoexcited electrons are injected into the conduction band, indicating that nitrogen is doped into the TiO_2 lattice, where it forms nitrogen-induced states. Fig. 5B shows the SPS of N719-sensitized N-doped and undoped ST-01 electrodes. The absorption band in the visible light region originates from the N719 dye that is adsorbed

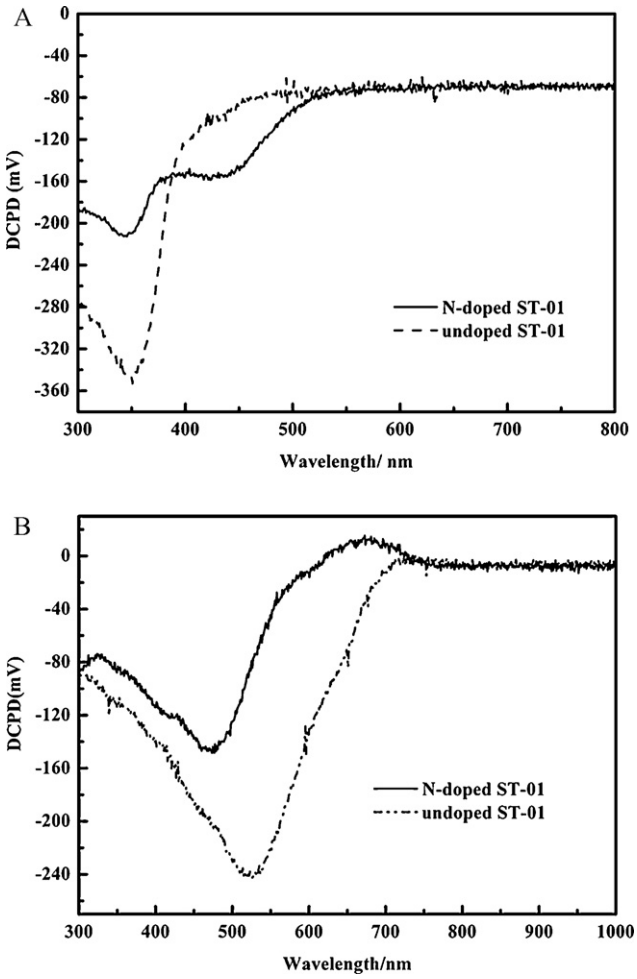

Fig. 5. Surface photovoltage spectra. Comparison of (A) N-doped and undoped ST-01 electrodes without dye, (B) N719-sensitized N-doped and undoped ST-01 electrodes.

on the TiO_2 particles. The decreasing light intensity from the lamp leads to a decrease in signal at short wavelengths. However, the observed signal for N-doped and undoped TiO_2 starting at around 740 nm (scanning from long to short wavelength) is due to the electron injection from the N719 dye into the conduction band of TiO_2. This electron injection leads to a photodoping effect, bringing about a change in E_F. However, the E_F under non-equilibrium (illumination) conditions becomes the quasi-Fermi level of the electrons ($E_{F,n}$). The result is that, under illumination, $(E_{CB} - E_{F,n}) < (E_{CB} - E_F)$ in the dark, which can be measured as a decrease in the work function and detected as a negative ΔCPD [26]. However, the signal for dye-sensitized N-doped ST-01 with respect to the undoped ST-01 is blue-shifted at about 20–40 nm. In general, this blue shift can be ascribed into two ways: Firstly, Grätzel and Cahen et al. observed a blue-shift for cells with Nb_2O_5 and $SrTiO_3$ compared with those with TiO_2. They suggested that the blue shift is due to electron injection from excited-state dye levels above the LUMO, below the E_{CB} of these semiconductors [26]. Secondly, the shift of the electron quasi-Fermi level in N-doped TiO_2. However, results of the change of Fermi level in N-doped TiO_2 are still unclear. Hashimoto et al. studied the flatband potentials of N-doped TiO_2 tend to shift to the positive direction [33]. Moreover, Kisch et al. observed that the quasi-Fermi level of electrons is anodically shifted by 0.07–0.16 eV [34]. However, the recent results disagree with the earlier conclusions. Higashimoto et al. reported that the flatband potential of N-doped TiO_2 is not influenced by small amounts of nitrogen

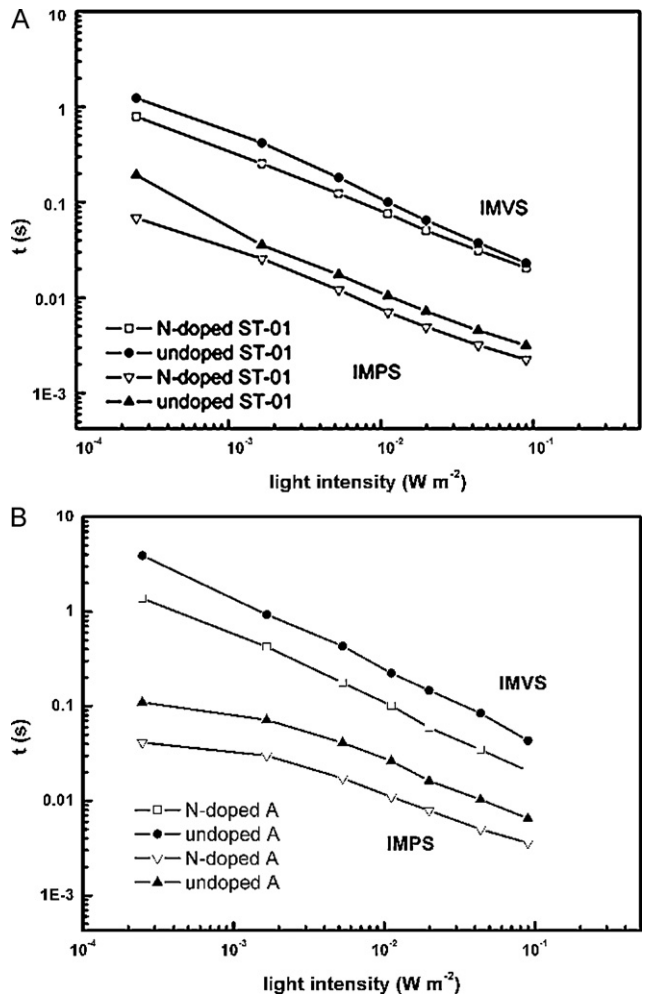

Fig. 6. IMPS and IMVS time constants as functions of light intensity for N719-sensitized (A) N-doped and undoped ST-01 solar cells, and (B) N-doped and undoped A solar cells with electrolytes.

species doped into TiO_2 [35]. Recently, Dai et al. observed a higher photovoltage in the N-doped DSCs. They demonstrated the change in the flatband of N-doped TiO_2, leading to a higher open-circuit photovoltage in DSCs [36]. Moreover, lower recombination losses can also contribute to a higher photovoltage. Therefore, we deduce that several effects refer to the enhancement of the photovoltage.

3.5. Electron transport and electron lifetime of DSCs

Electron transport in the N-doped DSCs was studied using IMPS under short-circuit conditions [37–39], and electron lifetime was probed using IMVS under open-circuit conditions [39–41]. The IMPS time constant corresponds to the average time required for the electrons to reach the conductive glass substrate from the location where they are photogenerated, which is considered to be the transport time (τ_{tr}) [27]. The IMVS time constant from a modulated photovoltage at open-circuit conditions equals the electron lifetime (τ_e), which is the average time for recombination of an electron in TiO_2 with species in the electrolyte or adsorbed on TiO_2.

Fig. 6 shows the IMPS and IMVS time constant as a function of light intensity. The transport times in both N-doped and undoped ST-01 DSCs decrease as the light intensity increases. However, a decrease in the transport time exists for the N-doped ST-01 DSC compared with the undoped DSC, which means faster electron transport in the N-doped TiO_2 films. A trapping model is generally used to explain electron transport in nanostructured TiO_2 [42]. Most electrons proceed with thousands of trapping/detrapping processes during transport to a conductive glass. While the charge trap sites can be formed by crystal defects and impurities, these trap sites are located mainly on the surface of the particles. However, the surface properties of TiO_2 appear to be changed due to nitrogen doping. In our previous work, the substitution of the oxygen sites with nitrogen atoms in the TiO_2 structure was confirmed by X-ray photoelectron spectroscopy [21]. Furthermore, the oxygen deficiency can also be filled by nitrogen, which contributes to a decrease in charge trap sites. However, the conditions of grain boundaries also influence the electron transport, especially in the nanoporous films [43]. When the particle size becomes nano-size, the volume ratio of boundaries to particles cannot be ignored. The electrons have to cross less grain boundaries for the bigger particle size of N-doped ST-01 as described above. Therefore, a faster electron transport can be observed in N-doped ST-01 DSCs. Moreover, Zhang et al. had reported that N-doped TiO_2 has introduced extra pathways for the charge carriers that could be beneficial for overall charge transport and thereby cell performance by introducing N-doped TiO_2 to form CdSe quantum-dot sensitized solar cell [44].

In Fig. 6, we can see that the electron lifetime, τ_e, in both N-doped and undoped TiO_2 films decreases as the light intensity increases. However, the electron lifetime becomes shorter in the N-doped ST-01 DSCs than in the undoped DSCs. As reported by Yanagida et al., the electron lifetime decreases as the particle size increases [45]. Accordingly, the bigger particle size of N-doped ST-01 causes a shorter lifetime in our case. When similar particle sizes of N-doped and undoped TiO_2 were used in DSCs, a longer lifetime was observed by Dai et al. They reported that N-doped TiO_2 photoelectrodes are able to successfully retard charge recombination [35]. However, we prepared similar particle size of N-doped A and undoped A by wet methods. Faster electron transport and shorter electron lifetime were observed from N-doped and undoped A DSCs, which confirmed the results we got from N-doped and undoped ST-01 DSCs.

For an efficient solar cell, the electron transport time must be significantly shorter than the electron lifetime. Based on Fig. 6, the lifetime, τ_e, is approximately one order of magnitude larger than the transport time, τ_{tr}, indicating that electron transport plays a key role in acquiring high collection efficiency for electron transfer in DSCs. Therefore, one can speculate that the faster electron transport in the N-doped TiO_2 film contributes to the higher energy conversion efficiency of DSCs based on N-doped TiO_2 electrode.

3.6. Stability test of the dye and the N-doped DSCs

Whether introducing N-doped TiO_2 to a DSC system can possibly accelerate the deterioration of the dye or not has always been a matter of concern. The results of the stability test for N-doped DSCs have been shown in our previous work, including the energy conversion efficiency and *Voc* during irradiation for 2000 h under white light (100 mW/cm^2) at 25 °C. Photodegradation was not observed for the N-doped DSC [21]. In order to further investigate the influence of the N-doped TiO_2 on the deterioration of the dye, stability tests of the dye adsorbed on the N-doped TiO_2 films and the photoelectrodes of the complete solar cells were performed.

As shown in Fig. 7(A) and Table 2, the absorption peaks of the N719 desorbed from the N-doped ST-01 and undoped ST-01 films are similar, although the same blue shift is observed in both cases compared with that of fresh N719. This is due to the photodegradation of N719 without the electron cycle in the electrolyte, as discussed in previous literature [46,47]. In addition, as shown in Fig. 7(B) for the two complete solar cells, the absorption peaks of N719 remain unchanged after exposure to sun-

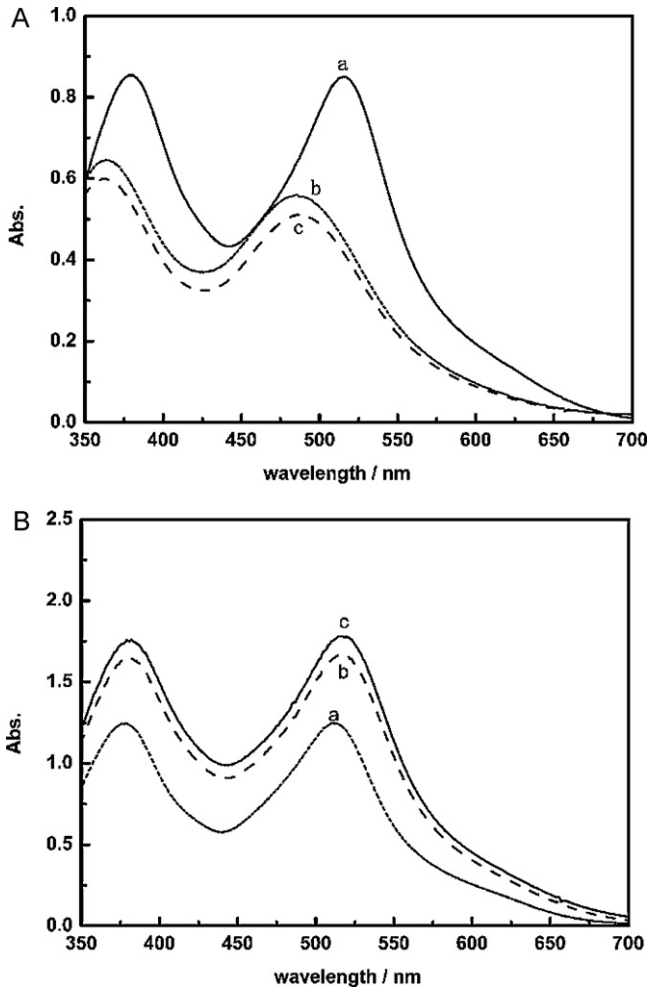

Fig. 7. UV–vis spectra. A: (a) fresh N719, (b) the N719 desorbed from the N-doped ST-01 film, (c) the N719 desorbed from the undoped ST-01 film. The films of (b) and (c) were stored in air for 4 years. B: (a) fresh N719, (b) the N719 desorbed from the N-doped ST-01 electrode, and (c) the N719 desorbed from the undoped ST-01 electrode. The solar cells of (b) and (c) were exposed to sunlight for 109 days.

light for 109 days. The result implies that the deterioration of the dye does not happen during the test period. In other words, the visible-light active N-doped TiO_2 does not accelerate the process of dye deterioration compared with the undoped TiO_2, an event ascribed to the introduction of nitrogen, which replaces oxygen deficiency in the TiO_2 crystal lattice. Dai et al. and our group have also performed stability tests on DSCs based on N-doped TiO_2 electrodes [21,35]. The results indicate that the N-doped DSCs possess excellent stability under light and at high temperature conditions (70 °C).

Table 2
Absorption data of N719 dye in the stability test analyzed by UV–vis spectra.

Samples in this work		λ^1_{max}	λ^2_{max}
Films	N-doped ST-01 (in air for 4 years)	363	489
	Undoped ST-01 (in air for 4 years)	365	489
Solar cells	N-doped ST-01 (under sunlight for 109 days)	380	516
	Undoped ST-01 (under sunlight for 109 days)	380	516
Dye solution	Fresh N719 in EtOH/NaOH/HCOOH solution	378	515

4. Conclusions

We have developed a series of DSCs based on N-doped and undoped TiO_2 electrodes. Needle-like N-doped TiO_2 crystals with excellent thermostability were simply prepared from the commercial TiO_2 powder. The N-doped DSCs successfully achieved a high energy conversion efficiency of 10.1% and 4.8% using an organic electrolyte and an ionic liquid $EMImBF_4$ electrolyte, respectively. Additionally, the starting TiO_2 materials for nitrogen doping are crucial for improving the energy conversion efficiency of DSCs. Moreover, N-doped DSCs possess higher photocurrent due to a higher dye uptake. Furthermore, an enhanced open circuit photovoltage was obtained in N-doped DSCs. The results of IMVS and IMPS showed a faster electron transport in the N-doped DSCs. Finally, the synergetic effect of higher dye uptake, faster electron transport and higher photovoltage contributes to a higher conversion efficiency of N-doped DSCs. In addition, the stability test of the N719-sensitized TiO_2 films and complete solar cells proved that N-doped TiO_2 does not accelerate dye degradation compared to undoped TiO_2. Therefore, N-doped TiO_2 nanocrystals prepared by our approach are ideal semiconductor materials for DSCs.

Acknowledgements

This research was supported by the National Natural Science Foundation of China (Grant No. 50773008) and State Key Laboratory of New Ceramic and Fine Processing (Tsinghua University). This work was also supported by the National High Technology Research and Development Program for Advanced Materials of China (Grant No. 2009AA03Z220) and the Program for Changjiang Scholars and Innovative Research Team in University (IRT0711).

Appendix A. Supplementary data

Supplementary data associated with this article can be found, in the online version, at doi:10.1016/j.jphotochem.2011.01.004.

References

[1] B. O'Regan, M. Grätzel, A low cost, high-efficiency solar cell based on dye-sensitized TiO_2 colloidal films, Nature 353 (1991) 737–740.
[2] M.K Nazeeruddin, A. Kay, I. Rodicio, R. Humphrey-Baker, E. Muller, P. Liska, N. Vlachopoulos, M. Grätzel, Conversion of light to electricity by cis-X_2Bis(2, 2′-bipyridyl-4, 4′-dicarboxylate)ruthenium(II) charge-transfer sensitizers (X = $C1^-$, Br^-, I^-, CN^-, and SCN^-) on nanocrystalline TiO_2 electrodes, J. Am. Chem. Soc. 115 (1993) 6382–6390.
[3] K. Sayama, H. Sugihara, H. Arakawa, Photoelectrochemical properties of a porous Nb_2O_5 electrode sensitized by a ruthenium dye, Chem. Mater. 10 (1998) 3825–3832.
[4] P. Guo, M.A. Aegerter, RU(II) sensitized Nb_2O_5 solar cell made by the sol–gel process, Thin Solid Films 351 (1999) 290–294.
[5] Q. Zhang, T.P. Chou, B. Russo, S.A. Jenekhe, G. Cao, Aggregation of ZnO nanocrystallites for high conversion efficiency in dye-sensitized solar cells, Angew. Chem. Int. Ed. 47 (2008) 2402–2406.
[6] J.F. Qian, P. Liu, Y. Xiao, Y. Jiang, Y.L. Cao, X.P. Ai, H. Yang, TiO_2-coated multilayered SnO_2 hollow microspheres for dye-sensitized solar cells, Adv. Mater. 21 (2009) 3663–3667.
[7] I. Shiyanovskaya, M. Hepel, Bicomponent WO_3/TiO_2 films as photoelectrodes, J. Electrochem. Soc. 146 (1999) 243–249.
[8] J. Moser, K. Brooks, M. Grätzel, Nanocrystalline mesoporous strontium titanate as photoelectrode material for photosensitized solar devices: increasing photovoltage through flatband potential engineering, J. Phys. Chem. B 103 (1999) 9328–9332.
[9] A. Turković, Z. Crnjak Orel, Dye-sensitized solar cell with CeO_2 and mixed CeO_2/SnO_2 photoanodes, Sol. Energy Mater. Solar Cells 45 (1997) 275–281.
[10] T. Lana-Villarreal, G. Boschloo, A. Hagfeldt, Nanostructured zinc stannate as semiconductor working electrodes for dye-sensitized solar cells, J. Phys. Chem. C 111 (2007) 5549–5556.
[11] B. Tan, E. Toman, Y. Li, Y. Wu, Zinc stannate (Zn_2SnO_4) dye-sensitized solar cells, J. Am. Chem. Soc. 129 (2007) 4162–4163.
[12] Y. Hu, Z. Zheng, H. Jia, Y. Tang, L. Zhang, Selective synthesis of FeS and FeS_2 nanosheet films on iron substrates as novel photocathodes for tandem dye-sensitized solar cells, J. Phys. Chem. C 112 (2008) 13037–13042.

[13] P. Qin, M. Linder, T. Brinck, G. Boschloo, A. Hagfeldt, L. Sun, High incident photon-to-current conversion efficiency of p-type dye-sensitized solar cells based on NiO and organic chromophores, Adv. Mater. 21 (2009) 2993–2996.
[14] A. Nattestad, M. Ferguson, R. Kerr, Y.B. Cheng, U. Bach, Dye-sensitized nickel(II) oxide photocathodes for tandem solar cell applications, Nanotechnology 19 (2008) 295304.
[15] C. Kim, K. Kim, H.Y. Kim, Y.S. Han, Modification of a TiO_2 photoanode by using Cr-doped TiO_2 with an influence on the photovoltaic efficiency of a dye-sensitized solar cell, J. Mater. Chem. 18 (2008) 5809–5814.
[16] S. Lee, J.H. Noh, H.S. Han, D.K. Yim, D.H. Kim, J.K. Lee, J.Y. Kim, H.S. Jung, K.S. Hong, Nb-doped TiO_2: a new compact layer material for TiO_2 dye-sensitized solar cells, J. Phys. Chem. C 113 (2009) 6878–6882.
[17] I. Inakamura, N. Negishi, S. Kutsuna, T. Ihara, S. Sugihara, K. Takeuchi, Role of oxygen vacancy in the plasma-treated TiO_2 photocatalyst with visible light activity for NO removal, J. Mol. Catal. A: Chem. 161 (2000) 205–212.
[18] T. Ihara, M. Miyoshi, Y. Iriyama, O. Matsumoto, S. Sugihara, Visible-light-active titanium oxide photocatalyst realized by an oxygen-deficient structure and by nitrogen doping, Appl. Catal. B: Environ. 42 (2003) 403–409.
[19] H. Irie, Y. Watanabe, K. Hashimoto, Nitrogen-concentration dependence on photocatalytic activity of $TiO_{2-x}N_x$ powders, J. Phys. Chem. B 107 (2003) 5483–5486.
[20] M. Mrowetz, W. Balcerski, A.J. Colussi, M.R. Hoffmann, Oxidative power of nitrogen-doped TiO_2 photocatalysts under visible illumination, J. Phys. Chem. B 108 (2004) 17269–17273.
[21] T. Ma, M. Akiyama, E. Abe, Isao Imai, High-efficiency dye-sensitized solar cell based on a nitrogen-doped nanostructured titania electrode, Nano Lett. 12 (2005) 2543–2547.
[22] T. Ma, E. Abe, Z. Zhou, F. Tokuoka, Y. Ito, T. Ishii, Japan Patent No. 2005-93944.
[23] Z. Zhou, F. Tokuoka, Y. Ito, T. Ishii, Visible-light active titania photocatalyst of nanoparticle and slurry, Kagaku Souchi 10 (2003) 64–66.
[24] T. Ma, T. Kida, M. Akiyama, K. Inoue, S. Tsunematsu, K. Yao, H. noma, E. Abe, Preparation and properties of nanostructured TiO_2 electrode by a polymer organic-medium screen-printing technique, Electrochem. Commun. 5 (2003) 369–372.
[25] T. Lindgren, J.M. Mwabora, E. Avendano, J. Jonsson, A. Hoel, C.G. Granqvist, S.E. Lindquist, Photoelectrochemical and optical properties of nitrogen doped titanium dioxide films prepared by reactive DC magnetron sputtering, J. Phys. Chem. B 107 (2003) 5709–5716.
[26] F. Lenzmann, J. Krueger, S. Burnside, K. Brooks, M. Grätzel, D. Gal, S. Rühle, D. Cahen, Surface photovoltage spectroscopy of dye-sensitized solar cells with TiO_2, Nb_2O_5, and $SrTiO_3$ nanocrystalline photoanodes: indication for electron injection from higher excited dye states, J. Phys. Chem. B 105 (2001) 6347–6352.
[27] G. Boschloo, A. Hagfeldt, Activation energy of electron transport in dye-sensitized TiO_2 solar cells, J. Phys. Chem. B 109 (2005) 12093–12098.
[28] X. Fang, Z. Zhang, Q. Chen, H. Ji, X. Gao, Dependence of nitrogen doping on TiO_2 precursor annealed under NH_3 flow, J. Solid State Chem. 180 (2007) 1325–1332.
[29] Y. Zhao, X. Qiu, C. Burda, The effects of sintering on the photocatalytic activity of N-doped TiO_2 nanoparticles, Chem. Mater. 20 (2008) 2629–2636.
[30] X. Wang, Y. Yang, Z. Jiang, R. Fan, Preparation of TiN_xO_{2-x} photoelectrodes with NH_3 under controllable middle pressures for dye-sensitized solar cells, Eur. J. Inorg. Chem. (2009) 3481–3487.
[31] D. Cahen, G. Hodes, M. Grätzel, J.F. Guillemoles, I. Riess, Nature of photovoltaic action in dye-sensitized solar cells, J. Phys. Chem B 104 (2000) 2053–2059.
[32] L. Kronik, Y. Shapira, Surface photovoltage spectroscopy of semiconductor structures: at the crossroads of physics, chemistry and electrical engineerin, Surf. Interface Anal. 31 (2001) 954–965.
[33] H. Irie, S. Washizuka, Y. Watanabe, T. Kako, K. Hashimoto, Photoinduced hydrophilic and electrochemical properties of nitrogen-doped TiO_2 films, J. Electrochem. Soc. 152 (2005) 351–356.
[34] H. Kisch, S. Sakthivel, M. Janczarek, D. Mitoraj, A low-band gap, nitrogen-modified titania visible-light photocatalyst, J. Phys. Chem. C 111 (2007) 11445–11449.
[35] S. Higashimoto, M. Azuma, Photo-induced charging effect and electron transfer to the redox species on nitrogen-doped TiO_2 under visible light irradiation, Appl. Catal. B: Environ. 89 (2009) 557–562.
[36] H. Tian, L. Hu, C. Zhang, W. Liu, Y. Huang, L. Mo, L. Guo, J. Sheng, S. Dai, Retarded charge recombination in dye-sensitized nitrogen-doped TiO_2 solar cells, J. Phys. Chem. C 114 (2010) 1627–1632.
[37] F. Cao, G. Oskam, P. Searson, Electron transport in porous nanocrystalline TiO_2 photoelectrochemical cells, J. Phys. Chem. C 100 (1996) 17021–17027.
[38] L. Dloczik, O. Ileperuma, I. Lauermann, L.M. Peter, E.A. Ponomarev, G. Redmond, N.J. Shaw, I. Uhlendorf, Dynamic response of dye-sensitized nanocrystalline solar cells: characterization by intensity-modulated photocurrent spectroscopy, J. Phys. Chem. B 101 (1997) 10281–10289.
[39] A.C. Fisher, L.M. Peter, E.A. Ponomarev, A.B. Walker, K.G.U. Wijayantha, Intensity dependence of the back reaction and transport of electrons in dye-sensitized nanocrystalline TiO_2 solar cells, J. Phys. Chem. B 104 (2000) 949–958.
[40] G. Schlichthörl, S.Y. Huang, J. Sprague, A.J. Frank, Band edge movement and recombination kinetics in dye-sensitized nanocrystalline TiO_2 solar cells: a study by intensity modulated photovoltage spectroscopy, J. Phys. Chem. B 101 (1997) 8141–8155.
[41] G. Schlichthörl, N.G. Park, A.J. Frank, Evaluation of the charge-collection efficiency of dye-sensitized nanocrystalline TiO_2 solar cells, J. Phys. Chem. B 103 (1999) 782–791.
[42] G. Boschloo, L. Häggman, A. Hagfeldt, Quantification of the effect of 4-tert-butylpyridine addition to I^-/I_3^- redox electrolytes in dye-sensitized nanostructured TiO_2 solar cells, J. Phys. Chem. B 110 (2006) 13144–13150.
[43] M.J. Cass, F.L. Qiu, A.B. Walker, A.C. Fisher, L.M. Peter, Influence of grain morphology on electron transport in dye sensitized nanocrystalline solar cells, J. Phys. Chem. B 107 (2003) 113–119.
[44] T. López-Luke, A. Wolcott, L. Xu, S. Chen, Z. Wen, J. Li, E.D.L. Rosa, J.Z. Zhang, Nitrogen-doped and CdSe quantum-dot-sensitized nanocrystalline TiO_2 films for solar energy conversion applications, J. Phys. Chem. C 112 (2008) 1282–1292.
[45] S. Nakade, Y. Saito, W. Kubo, T. Kitamura, Y. Wada, S. Yanagida, Influence of TiO_2 nanoparticle size on electron diffusion and recombination in dye-sensitized TiO_2 solar cells, J. Phys. Chem. B 107 (2003) 8607–8611.
[46] F. Nour-Mohhamadi, S.D. Nguyen, G. Boschloo, A. Hagfeldt, T. Lund, Determination of the light-induced degradation rate of the solar cell sensitizer N719 on TiO_2 nanocrystalline particles, J. Phys. Chem. B 109 (2005) 22413–22419.
[47] H.G. Agrell, J. Lindgren, A. Hagfeldt, Degradation mechanisms in a dye-sensitized solar cell studied by UV–vis and IR spectroscopy, Sol. Energy 75 (2003) 169–180.